

# Spiky oscillations in NF- $\kappa$ B signalling

Sandeep Krishna,\* Mogens H. Jensen, Kim Sneppen

Niels Bohr Institute, Blegdamsvej 17, 2100 Copenhagen Ø, Denmark.

\*To whom correspondence should be addressed; E-mail: sandeep@nbi.dk.

bioRxiv preprint doi: <https://doi.org/10.1101/009017>; this version posted September 4, 2005.

The NF- $\kappa$ B signalling system is involved in a variety of cellular processes including immune response, inflammation, and apoptosis. Recent experiments have found oscillations in the nuclear-cytoplasmic translocation of the NF- $\kappa$ B transcription factor [Hoffmann *et al.* (2002) *Science* 298, 1241; Nelson *et al.* (2004) *Science* 306, 704.] How the cell uses the oscillations to differentiate input conditions and send specific signals to downstream genes is an open problem. We shed light on this issue by examining the small core network driving the oscillations, which, we show, is designed to produce periodic spikes in nuclear NF- $\kappa$ B concentration. The oscillations can be used to regulate downstream genes in a variety of ways. In particular, we show that genes to whose operator sites NF- $\kappa$ B binds and dissociates fast can respond very sensitively to changes in the input signal, with effective Hill coefficients in excess of 20.

NF- $\kappa$ B is a family of dimeric transcription factors which participate in the regulation of a number of cellular processes including immune response, inflammation and apoptosis [1, 2, 3, 4]. Extensive experiments using electrophoretic mobility shift assay and single-cell fluorescence imaging have found oscillations in the nuclear-cytoplasmic translocation of the NF- $\kappa$ B transcription factor in mammalian cells [5, 6], with a time period of the order of hours. NF- $\kappa$ B can be activated by a number of external stimuli [7] including bacteria, viruses and various stresses and proteins (e.g., tumor necrosis factor- $\alpha$ , TNF- $\alpha$ , which was the signal used in refs. [5, 6]). In response to these signals it targets over 150 genes including many chemokines, immunoreceptors, stress response genes, as well as acute phase inflammation response proteins [7]. Experiments show that NF- $\kappa$ B does not regulate all its downstream genes in the same way. For example, the chemokine gene RANTES turns on much later than another chemokine IP-10 after TNF- $\alpha$  activation [5]. Thus, the two main questions raised by the dynamics of the NF- $\kappa$ B system are: how does the network of interactions produce oscillations, and how does the cell use the oscillations to differentiate input conditions and send specific signals to downstream genes? In this paper, we elucidate the small core network driving the oscillations and show that it is designed to produce periodic spikes in nuclear NF- $\kappa$ B concentration. We show that the spiky oscillations are extremely

robust to variation of parameters. We further argue that the spikiness is associated with an increased sensitivity of the system that could be used for differentially regulating downstream genes.

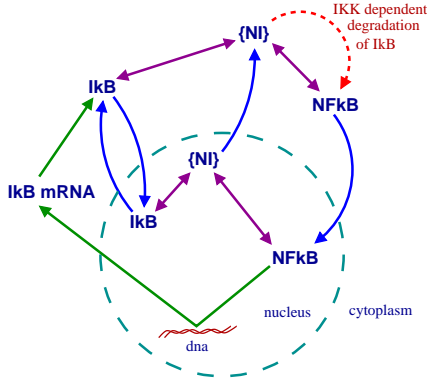
## Extracting the Core Feedback Loop

Hoffman *et al.* have constructed a long list of chemical reactions between 26 different molecules in the NF- $\kappa$ B system, including reaction constants [5]. We reduced this system to the core feedback loop (Fig. 1B) generating oscillations. The reduction was done in three steps: the first, removing molecules which have no feedback from NF- $\kappa$ B and deleting slow reactions where faster alternate pathways exist (e.g., export of nuclear NF- $\kappa$ B) resulted in a 7-variable model.

The interactions in this model are schematically displayed in Fig. 1A. It consists of cytoplasmic and nuclear NF- $\kappa$ B, its inhibitor, I $\kappa$ B, and I $\kappa$ B kinase (IKK) which phosphorylates the inhibitor, leading to its degradation. The inhibitor forms a complex with NF- $\kappa$ B which, in the cytoplasm, prevents its transport into the nucleus. Only free nuclear NF- $\kappa$ B is imported into the nucleus. In contrast, from inside the nucleus, only the complex can be exported, not the free NF- $\kappa$ B. I $\kappa$ B is known to occur in several isoforms. Cells containing only the I $\kappa$ B $\alpha$  isoform show sustained oscillations, while cells with only the I $\kappa$ B $\beta$  or  $\epsilon$  isoforms do not show oscillations. Wild type cells, with all three isoforms, typically exhibit damped oscillations [5]. The difference between these isoforms is that only I $\kappa$ B $\alpha$  is activated by NF- $\kappa$ B [8, 9]. In contrast I $\kappa$ B $\beta$ ,  $\epsilon$  are produced at a rate independent of NF- $\kappa$ B and so lie outside the feedback loop (see supporting text for the equations governing the dynamics of the 7-variable model.)

Coarse graining over fast chemical reactions involving complex formation reduced this system to 4 variables. Finally, based on numerical observations, we found we could effectively eliminate nuclear I $\kappa$ B, giving the model in Fig. 1B. More details of the reduction process are given in supporting text.

A



B

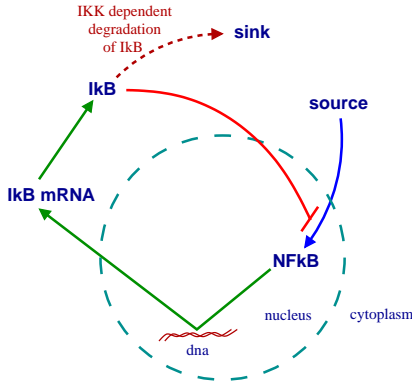


Figure 1: Schematic diagram of interactions in the NF- $\kappa$ B signalling system. **A.** 7-variable model. **B.** 3-variable model.

## Results

### 3-Variable Model of NF- $\kappa$ B Oscillations

The core feedback loop, we find, consists of only three constituents (Fig. 1B): nuclear NF- $\kappa$ B ( $N_n$ ), cytoplasmic I $\kappa$ B ( $I$ ) and I $\kappa$ B mRNA ( $I_m$ ). NF- $\kappa$ B dimers activate production of I $\kappa$ B mRNA which translated to I $\kappa$ B inhibits nuclear NF- $\kappa$ B production, completing the feedback loop.

The dynamics of the system in Fig. 1B is captured by three coupled ordinary differential equations:

$$\frac{dN_n}{dt} = A \frac{(1 - N_n)}{\epsilon + I} - B \frac{IN_n}{\delta + N_n}, \quad (1a)$$

$$\frac{dI_m}{dt} = N_n^2 - I_m, \quad (1b)$$

$$\frac{dI}{dt} = I_m - C \frac{(1 - N_n)I}{\epsilon + I}. \quad (1c)$$

For ease of analysis we have rescaled all variables to be dimensionless (the original equations and the rescaling process are described in supporting text.)  $A, B, C, \delta, \epsilon$  are dimensionless parameters dependent on the reaction constants (see supporting text). The external signal is supplied by IKK that enters the equations through the parameter,  $C$ , which is proportional to IKK concentration. The model has no spatial degrees of freedom. It has been suggested that flow induced stresses can trigger NF- $\kappa$ B mediated gene ac-

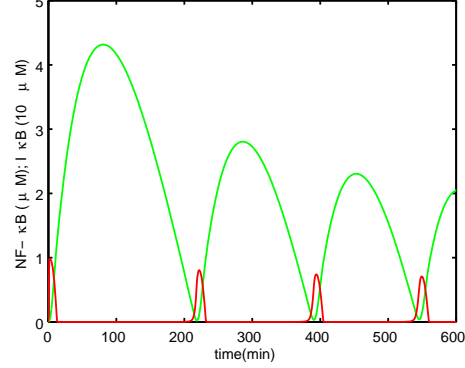


Figure 2: Sustained oscillations of nuclear NF- $\kappa$ B ( $N_n$ ), red, and cytoplasmic I $\kappa$ B, green, for  $A = 0.007$ ,  $B = 954.5$ ,  $C = 0.035$ ,  $\delta = 0.029$  and  $\epsilon = 2 \times 10^{-5}$  (using parameter values taken from [5], see supporting text). The shape, phase and period are remarkably similar to the experimental plot in Fig. 3B, left panel, in ref. [6].

tivity [10] but here we assume that each compartment, the cytoplasm and nucleus, is well-mixed.

The first term in equation (1a) represents the import of free cytoplasmic NF- $\kappa$ B (whose concentration is  $1 - N_n$ ) into the nucleus. This is hindered by the presence of cytoplasmic I $\kappa$ B which sequesters NF- $\kappa$ B in the cytoplasm. Parameter  $A$  is proportional to the NF- $\kappa$ B nuclear import rate. The second term in (1a) derives from the export of NF- $\kappa$ B from the nucleus via the NF- $\kappa$ B-I $\kappa$ B complex, which is why the term also depends on  $I$ .  $B$  is proportional to I $\kappa$ B nuclear import rate.  $\delta$  sets the concentration at which half the nuclear I $\kappa$ B is complexed to NF- $\kappa$ B and it depends both on the rates of association and dissociation of the complex as well as the export rate.

The first term in equation (1b), the rate of production of I $\kappa$ B mRNA, contains the square of  $N_n$  because the production is activated by NF- $\kappa$ B dimers<sup>†</sup>. The second term is the degradation of the mRNA whose rate, in these rescaled equations, sets the overall timescale. It is easy to modify this equation to deal with the  $\beta$  and  $\epsilon$  isoforms of I $\kappa$ B simply by adding a constant for their NF- $\kappa$ B-independent rate of production.

Equation (1c) has one term for the production of cytoplasmic I $\kappa$ B from its mRNA and a second for its degradation due to the presence of IKK. This degradation is proportional to the concentration of the NF- $\kappa$ B-I $\kappa$ B complex, which depends on both  $I$  and  $(1 - N_n)$ , the concentration of cytoplasmic NF- $\kappa$ B.  $\epsilon$  sets the concentration at which half of the cytoplasmic NF- $\kappa$ B is in the complex.  $C$  is proportional to the rate of degradation and to the IKK concentration.

Fig. 2 shows a plot of nuclear NF- $\kappa$ B and cytoplasmic I $\kappa$ B concentrations obtained in simulations, using parameter values from ref. [5]. Our model predicts the following experimentally observed facts [5, 6]: i) sustained oscillations in cells with only the  $\alpha$  isoform of I $\kappa$ B, ii)

<sup>†</sup>Ref. [11] argues that making this term linear in  $N_n$  is better. We have checked that this change does not alter our conclusions (see supporting text.)

damped oscillations in wild type cells which include other isoforms of  $I\kappa B$ , iii) time period of the order of hours, iv) spikiness of nuclear NF- $\kappa B$  and asymmetry of cytoplasmic  $I\kappa B$  oscillations, v) phase difference between NF- $\kappa B$  and  $I\kappa B$ , vi) lower frequency upon increased transcription of  $I\kappa B$ .

## Saturated Degradation of $I\kappa B$ is Crucial for Oscillations

A key element in our 3-variable model is the saturated degradation of cytoplasmic  $I\kappa B$  in the presence of IKK (second term in eq. 1c) due to the Michaelis-Menten complex formation between NF- $\kappa B$  and  $I\kappa B$  – a complex needed for IKK triggered degradation of  $I\kappa B$ . The same complex inhibits nuclear NF- $\kappa B$  production because only free cytoplasmic NF- $\kappa B$  is imported into the nucleus.

A stability analysis of the system shows the importance of the saturated degradation for oscillations. In general, the system has a single fixed point where all concentrations are unchanging in time. For small values of  $\epsilon$ , corresponding to strong saturation of the degradation, this fixed point is unstable and the system goes into a periodic cycle. As  $\epsilon$  is increased the fixed point becomes stable and the oscillations disappear (Fig. 3). This happens when the value of  $\epsilon$  becomes comparable to the steady state value of  $I$ , which is precisely when the degradation rate stops being saturated. The saturation is crucial for oscillations because it puts an upper limit to the degradation rate, allowing  $I\kappa B$  to accumulate and stay around longer than with the more usual  $I$ -proportional degradation rate. This effectively introduces a time delay into the feedback loop. Negative feedback with time delay is known to easily produce oscillations, and this mechanism has been used to model the p53 [12] and Hes oscillations [13]. Here, instead of being put in by hand, the time delay arises more naturally through the dynamics of the system.

Interestingly, the NF- $\kappa B$  core in Fig. 1B is similar to an early model showing oscillations by negative feedback [14] which introduced precisely the same kind of saturated degradation to mitigate the unreasonably large Hill coefficient in an even earlier model of Goodwin [15]. The importance of this mechanism has also been recognized by Goldbeter who has used it in models of various cellular oscillations, e.g., the cell cycle [16], development in myxobacteria [17], yeast stress response [18] and the mammalian circadian clock [19]. Saturated degradation has also been implicated in models of calcium oscillations in cells [20, 21]. We further note the p53 system, which also shows oscillations, contains the degradation of p53 via the formation of a complex with Mdm2 [22], which could result in saturated degradation. This suggests that saturated degradation might be a very general mechanism, easily implemented by complex formation and used by cellular processes to introduce time delays where necessary.

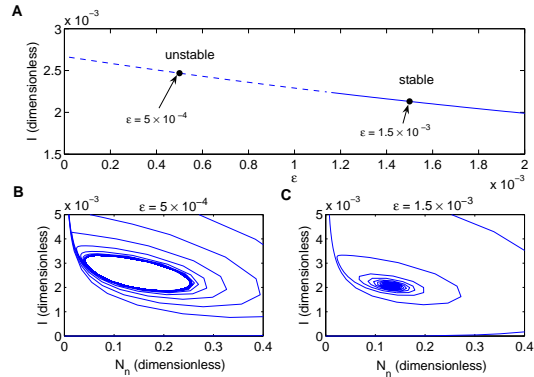


Figure 3: Importance of saturated degradation of  $I$ . **A.** Steady state solution of equation (1) for  $I$  as a function of the parameter  $\epsilon$ . Dashed line shows the region where the fixed point is unstable and the solid line shows the region where it is stable (see supporting text). Black dots mark the parameter values used in (B) and (C). The crossover from unstable to stable occurs where  $\epsilon$  becomes comparable to the steady state value of  $I$ , i.e., where the degradation of  $I$  stops being saturated. **B.** Trajectory of the system in the  $I$ - $N_n$  phase plane, for  $\epsilon = 5 \times 10^{-4}$ , which converges to a stable limit cycle. **C.** Trajectory of the system, for  $\epsilon = 1.5 \times 10^{-3}$ , which converges to a stable fixed point.

## Spiky Oscillations and Control of Downstream Genes

**Robust spiky oscillations.** One feature of our model is that it can produce sharp spikes in nuclear NF- $\kappa B$ . This is unusual for oscillations driven by negative feedback [23]. We quantify spikiness using the following measure:  $Z = (\max(N_n) - \min(N_n)) / \text{mean}(N_n)$ . Oscillations with  $Z > 2$  we term spiky, and oscillations with  $Z < 2$ , soft. Fig. 4 shows an example of each type of oscillation, generated from the 3-variable model using different parameter values.

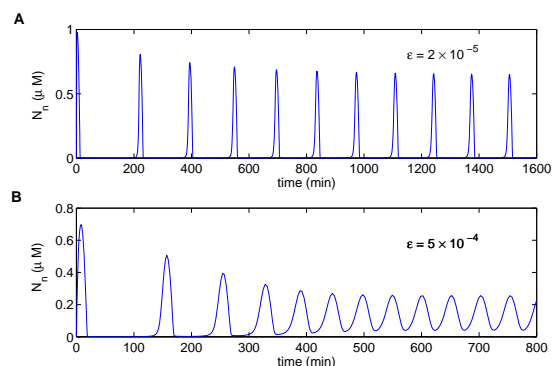
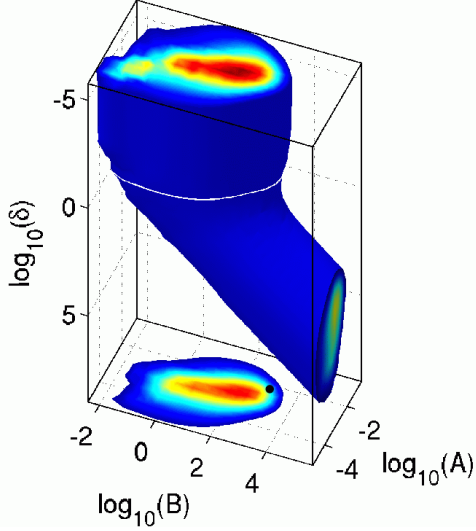


Figure 4: Spiky and soft oscillations. Plots of nuclear NF- $\kappa B$  concentration as a function of time from equation (1) with  $A, B, C$  and  $\delta$  the same as in Fig. 2. **A.** Spiky oscillations with  $\epsilon = 2 \times 10^{-5}$ , the same as in Fig. 2. **B.** Soft oscillations with  $\epsilon = 5 \times 10^{-4}$ .

The spikiness is extremely robust to variation of parameters as shown in Fig. 5. Note the scales are logarithmic: parameters can be varied by several decades without going out of the oscillatory regime. The enormous robustness suggests that the spikiness of the oscillations is an important element in the design of NF- $\kappa$ B signalling and may be essential for its proper functioning as a transcription factor. We substantiate this idea in the subsequent sections.

A



B

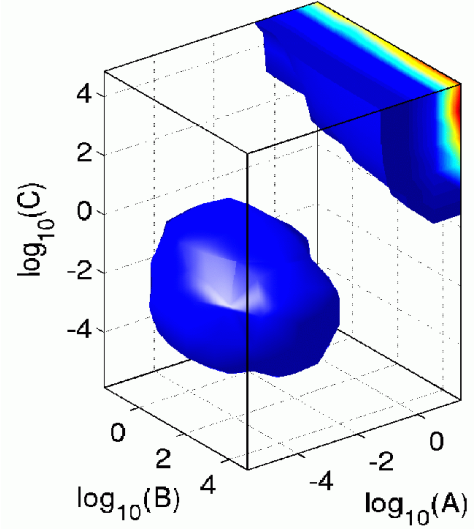


Figure 5: Robustness of spiky oscillations. The 3d volume is the region of spiky oscillations ( $Z > 2$ , defined in main text); colour gradient towards red shows increasing values of  $Z$ . **A.** The robustness for parameters  $A, B, \delta$ . The 2d plot shows the horizontal slice (white line) through the 3d volume at  $\delta = 0.029$ , the value used in Fig. 2. The black dot corresponds to values of  $A, B$  used in Fig. 2. **B.** A similar plot for parameters  $A, B, C$ .

### Sensitivity to IKK is high for spiky oscillations.

Since IKK is the external signal to which the system responds, we begin by comparing the sensitivity of spiky and soft oscillations to changes in IKK concentration. We consider two quantities: the spike duration, defined as the amount of time  $N_n$  spends above its average value, and the spike peak, defined as the maximum nuclear NF- $\kappa$ B concentration during each cycle of oscillations. Fig. 6A shows how the spike duration depends on IKK concentration. The sensitivity of the spike duration is very high in certain regions of spiky oscillations. It is especially large near the transition to soft oscillations. A similar sensitivity is seen in the peak NF- $\kappa$ B concentration (Fig. 6B). Thus, the spike duration and peak are much more sensitive to (and therefore easier to regulate by) IKK for spiky than for soft oscillations.

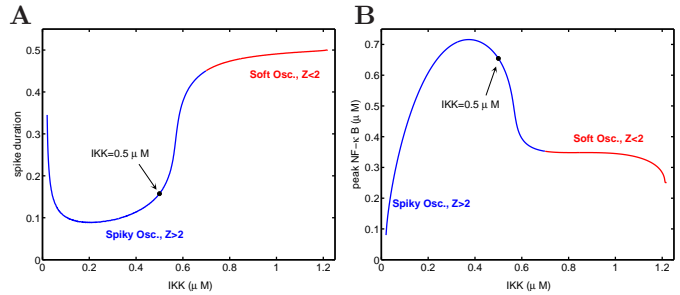
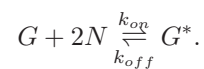


Figure 6: Sensitivity to IKK. **A.** Spike duration, the fraction of time  $N_n$  spends above its mean value, as a function of IKK concentration. The black dot shows the IKK value used in Fig. 2. Blue and red signify, respectively, regions of spiky and soft oscillations. Notice the sharp response just before the transition to soft oscillations. **B.** Spike peak, the maximum concentration of nuclear NF- $\kappa$ B, as a function of IKK concentration. The black dot shows the IKK value used in Fig. 2. Blue and red signify, respectively, regions of spiky and soft oscillations. Notice the sharp response just before the transition to soft oscillations.

**Large Hill coefficients and regulation of downstream genes.** It is possible for genes regulated by NF- $\kappa$ B to inherit this sensitivity in the form of a high effective Hill coefficient. Consider a gene which has an operator site at which NF- $\kappa$ B dimers can bind and activate the gene:



To begin with, we assume that the binding of NF- $\kappa$ B to the operator is in equilibrium, i.e.,  $k_{on}$  and  $k_{off}$  are much larger

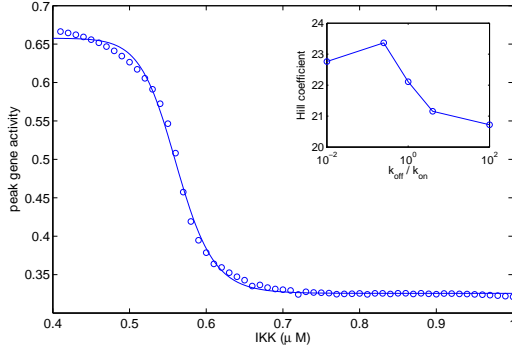


Figure 7: Equilibrium binding of NF- $\kappa$ B to a downstream gene. The plot shows the peak gene activity as a function of IKK concentration (open circles). The data has been fitted by a sigmoidal function of the form  $1/(1 + (x/x_0)^h)$ . The least squares fit (solid line) gives an effective Hill coefficient  $h = 23.4$ . Inset: effective Hill coefficient obtained by similar fitting for different  $k_{off}/k_{on}$  ratios.

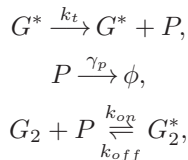
than the rates of all other processes in the NF- $\kappa$ B system. In that case the gene activity,  $G^*$ , will follow the NF- $\kappa$ B concentration:

$$G^* = \frac{N_n^2}{k_{off}/k_{on} + N_n^2}.$$

Fig. 7 shows the peak gene activity as a function of IKK concentration. The effective Hill coefficient of this response curve is over 20, much larger than the values obtained by typical ways of introducing cooperativity in gene regulation [24, 25]. As the inset shows, the effective Hill coefficient remains above 20 for a large range of values of the ratio  $k_{off}/k_{on}$ , i.e., genes controlled in this way show a very high sensitivity to the input signal.

When  $k_{on}$  and  $k_{off}$  become comparable to other rates in the system the binding of NF- $\kappa$ B to the operator remains out of equilibrium. When  $k_{off}$  is small enough, the gene activity does not have enough time to decay completely between spikes of NF- $\kappa$ B. Fig. 8 shows the peak activity as a function of IKK. In contrast to the equilibrium case, here the response is linear at best. Note also that the peak gene activity increases with IKK in contrast to the equilibrium case where it decreases. Thus, the same oscillations are capable of regulating genes very differently, depending on their  $k_{on,off}$  values which are determined by their operator sites.

In the extreme case where  $k_{off}$  is negligible, each spike of nuclear NF- $\kappa$ B contributes to increase the gene activity until it saturates to unity as shown by the solid line in Fig. 9. If this gene controls the activity of a second one in a cascade:



then the latter will turn on later (dashed line in Fig. 9) with a time delay that depends on the timescales of transcription,

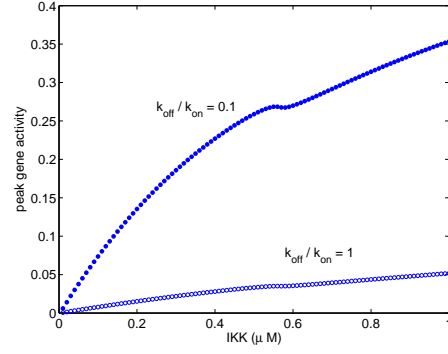


Figure 8: Nonequilibrium binding of NF- $\kappa$ B to a downstream gene. The plot shows the peak gene activity as a function of IKK concentration, with  $k_{off} = 0.001 \text{ min}^{-1}$  kept fixed while  $k_{on} = 0.01 \mu\text{M}^{-1} \text{ min}^{-1}$  for filled circles and  $0.001 \mu\text{M}^{-1} \text{ min}^{-1}$  for open circles.

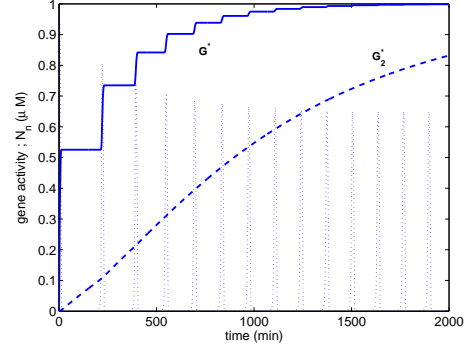


Figure 9: Strongly nonequilibrium binding of NF- $\kappa$ B to a downstream gene. The plot shows nuclear NF- $\kappa$ B concentration (dotted line), the activity of a gene,  $G^*$  (solid line), directly activated by NF- $\kappa$ B dimers with  $k_{on} = 0.1 \mu\text{M}^{-2} \text{ min}^{-1}$ ,  $k_{off} = 0$ , and the activity of a second gene,  $G_2^*$  (dashed line), that is activated by the protein product of  $G$  ( $k_t = 0.01 \text{ min}^{-1}$ ,  $\gamma_p = 1 \text{ min}^{-1}$ , see main text).

translation and promoter activation. This is reminiscent of the experiments of ref. [5] which show the gene IP-10 turning on quickly after the introduction of IKK, while the gene RANTES turns on after a delay.

## Discussion

What functional role, if any, do the oscillations in the NF- $\kappa$ B system play? There have been several suggestions: downstream gene networks are perhaps regulated by the frequency of the oscillations, or the oscillations could be a by-product of rapid attenuation of NF- $\kappa$ B, or they might be used to make multiple evaluations of the input signal [26, 27]. Barken *et al.* [28] warn against overemphasising the physiological role of oscillations. Our approach to tackling this question has been to construct a reduced 3-variable model which, despite its simplicity, captures many charac-



teristic features of the system. The simplicity of the model allows us to fully explore and understand the range of dynamical behaviour it exhibits. In particular, we have shown that it is capable of both spiky and soft oscillations, and that the spiky oscillations are extremely robust to variation of parameters.

The activity of genes downstream of NF- $\kappa$ B depends upon the amount of time for which NF- $\kappa$ B is present inside the nucleus in sufficiently large concentrations to dimerize and bind to those genes' operator sites. It seems reasonable to assume that NF- $\kappa$ B could signal different downstream genes, simply by regulating the amount and exposure time to IKK, provided the signalling system is sufficiently sensitive to changes in IKK concentration. We have shown that the spiky oscillations can, indeed, show a high sensitivity to IKK. This sensitivity allows a great versatility in the regulation of downstream genes by NF- $\kappa$ B. Where the cell requires a gene to be very sensitive to the IKK concentration, the NF- $\kappa$ B system can result in steep response curves with Hill coefficients larger than 20. And where a slower response is necessary, it can be achieved by adjusting the binding and dissociation constants of NF- $\kappa$ B to that operator site. Further, we found that cascades of different length could be used to turn certain genes on earlier or later. Given this versatility in regulatory strategies it seems likely that cells would have evolved to make use of these properties of the NF- $\kappa$ B oscillations. It remains for future experiments to uncover the particular ways NF- $\kappa$ B regulates specific genes.

We thank J. Ferkinghoff-Borg, E. Siggia and G. Tiana for useful discussions. This work was supported by the Danish Research Foundation.

## References

- [1] Lee, K.-Y., D'Acquisto, F., Hayden, M. S., Shima, J.-H. & Ghosh, S. (2005) *Science* **308**, 114–118.
- [2] Lawrence, P., Bebién, M., Liu, G. Y., Nizet, V. & Karin, M. (2005) *Nature* **434**, 1138–1143.
- [3] Ghosh, S. & Karin, M. (2002) *Cell* **109**, S81–S96.
- [4] Ghosh, S., May, M. J. & Kopp, E. B. (1998) *Annu. Rev. Immunol.* **16**, 225.
- [5] Hoffmann, A., Levchenko, A., Scott, M. L. & Baltimore, D. (2002) *Science* **298**, 1241.
- [6] Nelson, D. E., Ihekweaba, A. E. C., Elliott, M., Johnson, J. R., Gibney, C. A., Foreman, B. E., Nelson, G., See, V., Horton, C. A., Spiller, D. G. *et al.* (2004) *Science* **306**, 704.
- [7] Pahl, H. L. (1999) *Oncogene* **18**, 6853–6866.
- [8] Sun, S. C., Ganchi, P. A., Ballard, D. W. & Greene, W. C. (1993) *Science* **259**, 1912.
- [9] Scott, M. L., Fujita, T., Liou, H. C., Nolan, G. P. & Baltimore, D. (1993) *Genes Dev.* **7**, 1266.
- [10] Ganguli, A., Persson, L., Palmer, I. R., Evans, I., Yang, L., Smallwood, R., Black, R. & Qvarnstrom, E. E. (2005) *Circ. Res.* **96**, 1–9.
- [11] Nelson, D. E., Horton, C. A., See, V., Johnson, J. R., Nelson, G., Spiller, D. G., Kell, D. B. & White, M. R. H. (2005) *Science* **308**, 52b.
- [12] Tiana, G., Sneppen, K. & Jensen, M. H. (2002) *Eur. J. Phys. B* **29**, 135–140.
- [13] Jensen, M. H., Sneppen, K. & Tiana, G. (2003) *FEBS Lett.* **541**, 176–177.
- [14] Bliss, R. D., Painter, P. R. & Marr, A. G. (1982) *J. Theor. Biol.* **97**, 177.
- [15] Goodwin, B. C. (1965) in *Adv. Enzyme Regulation*, ed. Weber, G. (Pergamon Press, Oxford) Vol. 3, pp. 425–438.
- [16] Goldbeter, A. (1991) *Proc. Natl. Acad. Sci. (USA)* **88**, 9107.
- [17] Igoshin, O. A., Goldbeter, A., Kaiser, D. & Oster, G. (2004) *Proc. Natl. Acad. Sci. (USA)* **101**, 15760.
- [18] Jacquet, H., Renault, G., Lallet, S., Mey, J. D. & Goldbeter, A. (2003) *J. Cell Biol.* **161**, 497–505.
- [19] Leloup, J.-C. & Goldbeter, A. (2003) *Proc. Natl. Acad. Sci. (USA)* **100**, 7051–7056.
- [20] Reidl, J., Borowski, P., Sensse, A., Starke, J., Zapotocky, M. & Eiswirth, M. (2005) *Biophys. J.* in press.
- [21] Goldbeter, A., Dupont, G. & Berridge, M. (1990) *Proc. Natl. Acad. Sci. (USA)* **87**, 1461–1465.
- [22] Vogelstein, B., Lane, D. & Levine, A. J. (2000) *Nature* **408**, 307–310.
- [23] Goldbeter, A. (2002) *Nature* **420**, 238.
- [24] Huang, C.-Y. F. & Ferrel Jr., J. E. (1996) *Proc. Natl. Acad. Sci. (USA)* **93**, 10078–10083.
- [25] Goldbeter, A. & Koshland, D. E. (1981) *Proc. Natl. Acad. Sci. (USA)* **78**, 6840–6844.
- [26] Lahav, G. (2004) *Science's STKE*. pe55.
- [27] Ting, A. Y. & Endy, D. (2002) *Science* **298**, 1189–1190.
- [28] Barken, D., Wang, C. J., Kearns, J., Cheong, R., Hoffmann, A. & Levchenko, A. (2005) *Science* **308**, 52a.

## Supporting Text

### 7-variable model of NF- $\kappa$ B signalling

We use the following abbreviations:  $N_n$  &  $N$ , free nuclear and cytoplasmic NF- $\kappa$ B;  $I_m$ , I $\kappa$ B mRNA;  $I_n$  &  $I$ , free nuclear and cytoplasmic I $\kappa$ B;  $(NI)_n$  &  $(NI)$ , nuclear and cytoplasmic NF- $\kappa$ B-I $\kappa$ B complex; IKK, I $\kappa$ B kinase. The 7-variable model is defined by the equations:

$$\begin{aligned}\frac{dN_n}{dt} &= k_{Nin}N - k_{fn}N_nI_n + k_{bn}(NI)_n, \\ \frac{dI_m}{dt} &= k_tN_n^2 - \gamma_mI_m, \\ \frac{dI}{dt} &= k_{tl}I_m - k_fNI + k_b(NI) - k_{Iin}I + k_{Iout}I_n, \\ \frac{dN}{dt} &= -k_fNI + (k_b + \alpha)(NI) - k_{Nin}N, \\ \frac{d(NI)}{dt} &= k_fNI - (k_b + \alpha)(NI) + k_{NIout}(NI)_n, \\ \frac{dI_n}{dt} &= k_{Iin}I - k_{Iout}I_n - k_{fn}N_nI_n + k_{bn}(NI)_n, \\ \frac{d(NI)_n}{dt} &= k_{fn}N_nI_n - (k_{bn} + k_{NIout})(NI)_n.\end{aligned}$$

Figure S1 shows a plot of nuclear NF- $\kappa$ B concentration obtained by integrating these equations using the following parameter values (Hoffmann et al. (2002) *Science* **298**, 1241):  $k_{Nin} = 5.4 \text{ min}^{-1}$ ,  $k_{Iin} = 0.018 \text{ min}^{-1}$ ,  $k_{Iout} = 0.012 \text{ min}^{-1}$ ,  $k_{NIout} = 0.83 \text{ min}^{-1}$ ,  $k_t = 1.03 \mu M^{-1} \text{ min}^{-1}$ ,  $k_{tl} = 0.24 \text{ min}^{-1}$ ,  $k_f = k_{fn} = 30 \mu M^{-1} \text{ min}^{-1}$ ,  $k_b = k_{bn} = 0.03 \text{ min}^{-1}$ ,  $\alpha = 1.05 \times \text{IKK} \text{ min}^{-1}$ ,  $\gamma_m = 0.017 \text{ min}^{-1}$ . The initial conditions were  $N = 1 \mu M$ ,  $\text{IKK} = 0.5 \mu M$  and all other concentrations zero.

### Reduction from 7-variables to 3-variables

First, taking note of the fact that  $k_f$  and  $k_{fn}$  are large, we assume that all complexes are in equilibrium, i.e.:

$$k_fNI \approx (k_b + \alpha)(NI),$$

$$k_{fn}N_nI_n \approx (k_{bn} + k_{NIout})(NI)_n.$$

Simulations show that these are good approximations. In terms of  $I_n^{tot} \equiv I_n + (NI)_n$  and  $N_c^{tot} \equiv N + (NI) = N_{tot} - N_n$ , which are slowly varying, we can rewrite the above equations as follows:

$$(NI) = (N_{tot} - N_n) \frac{I}{K_I + I},$$

$$N = (N_{tot} - N_n) \frac{K_I}{K_I + I},$$

$$(NI)_n = I_n^{tot} \frac{N_n}{K_N + N_n},$$

$$I_n = I_n^{tot} \frac{K_N}{K_N + N_n},$$

where  $K_I \equiv (k_b + \alpha)/k_f = 0.035 \mu M$  and  $K_N \equiv (k_{bn} + k_{NIout})/k_{fn} = 0.029 \mu M$ , using the parameter values above.

Using these expressions, the equations of the 7-variable model reduce to the following four (Fig. S1):

$$\frac{dN_n}{dt} = k_{Nin}K_I \frac{(N_{tot} - N_n)}{K_I + I} - k_{NIout} \frac{I_n^{tot} N_n}{K_N + N_n},$$

$$\frac{dI_m}{dt} = k_t N_n^2 - \gamma_m I_m,$$

$$\frac{dI}{dt} = k_{tl} I_m - \alpha \frac{(N_{tot} - N_n) I}{K_I + I} - k_{Iin} I + k_{Iout} K_N \frac{I_n^{tot}}{K_N + N_n},$$

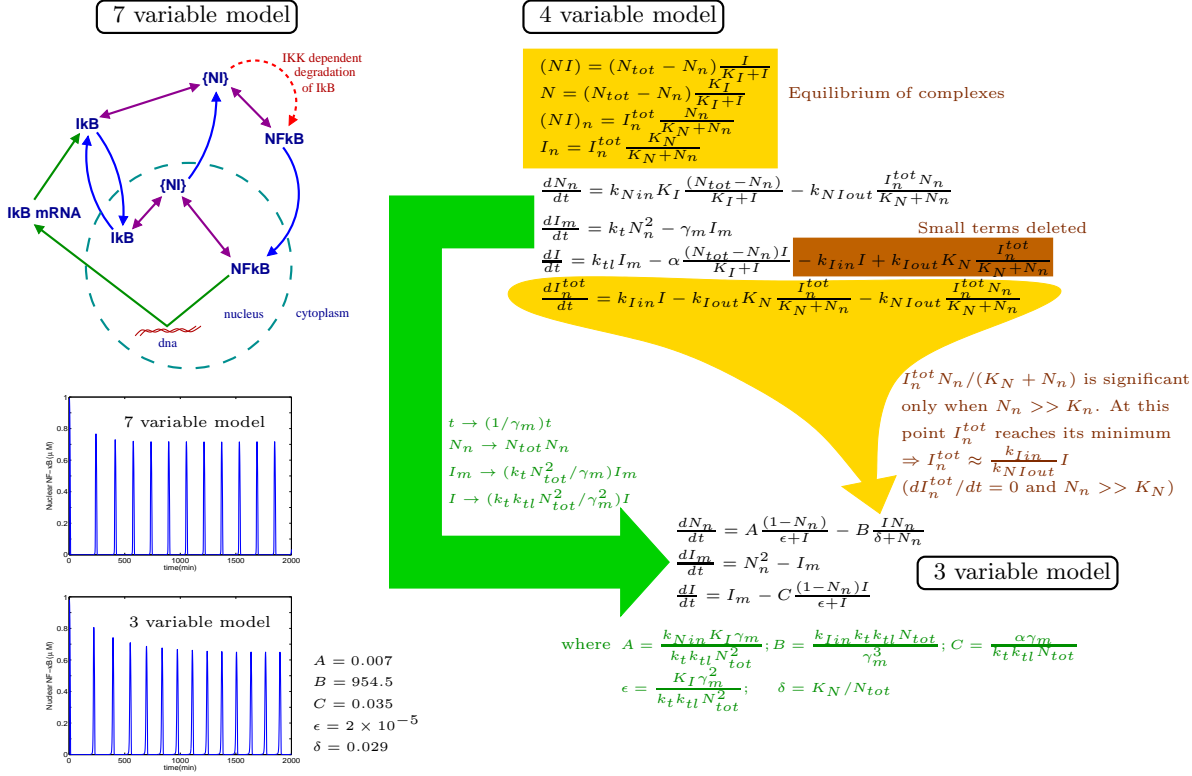


Figure S1: Schematic showing reduction of the 7-variable to a 3-variable model, as well as plots of oscillatory nuclear NF- $\kappa$ B from simulations of the 7 and 3-variable models using parameter values given in the text.

$$\frac{dI_n^{tot}}{dt} = k_{Iin} I - k_{Iout} K_N \frac{I_n^{tot}}{K_N + N_n} - k_{NIout} \frac{I_n^{tot} N_n}{K_N + N_n}.$$

First, we note that the terms  $-k_{Iin} I$  and  $k_{Iout} K_N \frac{I_n^{tot}}{K_N + N_n}$  in the  $dI/dt$  equation are much smaller than  $-\alpha \frac{(N_{tot} - N_n) I}{K_I + I}$  and can be neglected as long as IKK is non-zero. Secondly, simulations reveal that the term  $k_{NIout} \frac{I_n^{tot} N_n}{K_N + N_n}$ , in the  $dI_n^{tot}/dt$  equation, also shows sharp spikes as a function of time which coincide with the spikes of  $N_n$ . The value of this term is substantial only when  $N_n \gg K_N$ , i.e., during the spikes of  $N_n$ , and at those times  $I_n^{tot}$  dips to its minimum. We therefore make the approximation that  $I_n^{tot}$  can be replaced by its minimum value,  $I_{n,min}^{tot}$ , which satisfies the equation:

$$k_{Iin} I = k_{Iout} K_N \frac{I_{n,min}^{tot}}{K_N + N_n} + k_{NIout} \frac{I_{n,min}^{tot} N_n}{K_N + N_n}.$$

In the regime where  $N_n \gg K_n$  this gives

$$I_{n,min}^{tot} \approx \frac{k_{Iin}}{k_{NIout}} I.$$

Using this we can reduce to a 3-variable model:

$$\frac{dN_n}{dt} = k_{Nin} K_I \frac{(N_{tot} - N_n)}{K_I + I} - k_{Iin} \frac{I N_n}{\delta + N_n},$$

$$\frac{dI_m}{dt} = k_t N_n^2 - \gamma_m I_m,$$

$$\frac{dI}{dt} = k_{tl} I_m - \alpha \frac{(N_{tot} - N_n) I}{K_I + I}.$$

## Rescaling the 3-variable model

For ease of analysis, we reduce the number of parameters in the model by rescaling all variables to become dimensionless. We use the following transformations on the above equations:

$$t \rightarrow (1/\gamma_m)t,$$



$$\begin{aligned}
N_n &\rightarrow N_{tot}N_n, \\
I_m &\rightarrow (k_t N_{tot}^2 / \gamma_m) I_m, \\
I &\rightarrow (k_t k_{tl} N_{tot}^2 / \gamma_m^2) I,
\end{aligned}$$

which gives:

$$\begin{aligned}
\frac{dN_n}{dt} &= A \frac{(1 - N_n)}{\epsilon + I} - B \frac{IN_n}{\delta + N_n}, \\
\frac{dI_m}{dt} &= N_n^2 - I_m \\
\frac{dI}{dt} &= I_m - C \frac{(1 - N_n)I}{\epsilon + I},
\end{aligned}$$

with

$$\begin{aligned}
A &= \frac{k_{Nin} K_I \gamma_m}{k_t k_{tl} N_{tot}^2} \approx 0.007, \\
B &= \frac{k_{Iin} k_t k_{tl} N_{tot}}{\gamma_m^3} \approx 954.5, \\
C &= \frac{\alpha \gamma_m}{k_t k_{tl} N_{tot}} \approx 0.035, \\
\delta &= \frac{K_N}{N_{tot}} \approx 0.029, \\
\epsilon &= \frac{K_I \gamma_m^2}{k_t k_{tl} N_{tot}^2} \approx 2 \times 10^{-5}.
\end{aligned}$$

### Steady state solution of the 3-variable model

The steady state values of  $N_n$ ,  $I_m$  and  $I$  are solutions to

$$\begin{aligned}
A \frac{(1 - N_n)}{\epsilon + I} - B \frac{IN_n}{\delta + N_n} &= 0, \\
N_n^2 - I_m &= 0, \\
I_m - C \frac{(1 - N_n)I}{\epsilon + I} &= 0.
\end{aligned}$$

$I_m$  and  $I$  can be eliminated using

$$\begin{aligned}
I_m &= N_n^2, \\
I &= \frac{N_n^2 \epsilon}{C - CN_n - N_n^2}.
\end{aligned}$$

From this we find that the steady state value of  $N_n$  is a solution of the equation

$$(C - CN_n - N_n^2)^2 = \frac{BC\epsilon^2}{A} \frac{N_n^3}{\delta + N_n},$$

or equivalently,

$$N_n^5 + (\delta + 2C)N_n^4 + C \left[ 2(\delta - 1) + C - \frac{B}{A} \epsilon^2 \right] N_n^3 + C[(C - 2)\delta - 2C]N_n^2 + C^2(1 - 2\delta)N_n + C^2\delta = 0.$$

In general, this has two real solutions, one with  $C - CN_n - N_n^2 > 0$  and the other with  $C - CN_n - N_n^2 < 0$ . The latter results in a negative value for  $I$  and therefore is not an acceptable solution. Thus we are left with only one fixed point.

## Linear stability of the fixed point

We linearize the equations around the fixed point, which gives the Hessian

$$J = \begin{pmatrix} -\frac{A}{\epsilon+I} - \frac{\delta BI}{(\delta+N_n)^2} & 0 & -\frac{A(1-N_n)}{(\epsilon+I)^2} - \frac{BN_n}{\delta+N_n} \\ 2N_n & -1 & 0 \\ \frac{CI}{\epsilon+I} & 1 & -\frac{C\epsilon(1-N_n)}{(\epsilon+I)^2} \end{pmatrix}$$

This matrix can be used to examine the stability of the fixed point. If  $\lambda_i$  are the (possibly complex) eigenvalues of this matrix, then the fixed point is unstable if

$$\max_i [\text{Re}(\lambda_i)] > 0$$

and stable if

$$\max_i [\text{Re}(\lambda_i)] < 0.$$

## Linear production of $I_m$

In this section we consider the effect of taking the production of  $I_m$  to be linear in  $N_n$ , instead of  $N_n^2$ :

$$\frac{dN_n}{dt} = k_{Nin} K_I \frac{(N_{tot} - N_n)}{K_I + I} - k_{Iin} \frac{IN_n}{\delta + N_n},$$

$$\frac{dI_m}{dt} = k_t N_n - \gamma_m I_m,$$

$$\frac{dI}{dt} = k_{tl} I_m - \alpha \frac{(N_{tot} - N_n)I}{K_I + I}.$$

Using very similar transformations, we rescale the variables:

$$t \rightarrow (1/\gamma_m)t,$$

$$N_n \rightarrow N_{tot} N_n,$$

$$I_m \rightarrow (k_t N_{tot} / \gamma_m) I_m,$$

$$I \rightarrow (k_t k_{tl} N_{tot} / \gamma_m^2) I,$$

which gives:

$$\frac{dN_n}{dt} = A \frac{(1 - N_n)}{\epsilon + I} - B \frac{IN_n}{\delta + N_n},$$

$$\frac{dI_m}{dt} = N_n - I_m,$$

$$\frac{dI}{dt} = I_m - C \frac{(1 - N_n)I}{\epsilon + I},$$

with

$$A = \frac{k_{Nin} K_I \gamma_m}{k_t k_{tl} N_{tot}},$$

$$B = \frac{k_{Iin} k_t k_{tl}}{\gamma_m^3},$$

$$C = \frac{\alpha \gamma_m}{k_t k_{tl}},$$

$$\delta = \frac{K_N}{N_{tot}},$$

$$\epsilon = \frac{K_I \gamma_m^2}{k_t k_{tl} N_{tot}}.$$

If we use the same parameter values as before we do not get sustained oscillations. Not surprisingly, the region in parameter space where we get sustained oscillations has shifted. Simply taking  $A = 0.001$ , we get spiky oscillations, as in the original model (Fig. S2A). Fig. S2B shows the response to changes in IKK.

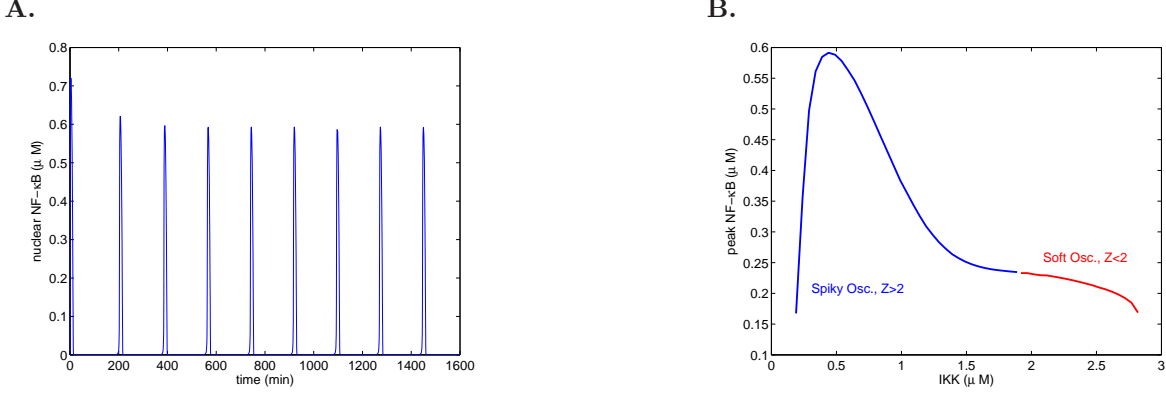


Figure S2: **A.** Sustained spiky oscillations of nuclear NF- $\kappa$ B when the production of  $I_m$  is linearly dependent on  $N_n$ . Parameter values:  $A = 0.001$ ,  $B = 954.5$ ,  $C = 0.035$ ,  $\delta = 0.029$  and  $\epsilon = 2 \times 10^{-5}$ . **B.** Spike peak, the maximum concentration of nuclear NF- $\kappa$ B, as a function of IKK concentration. Blue and red signify, respectively, regions of spiky and soft oscillations.

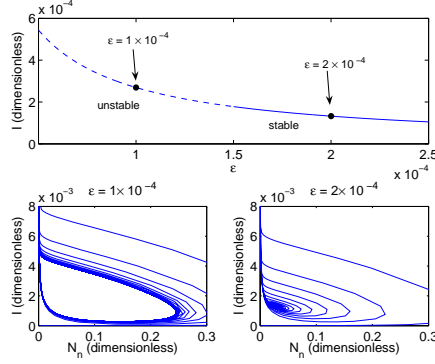


Figure S3: **A.** Steady state solution for  $I$  as a function of the parameter  $\epsilon$ , when the production of  $I_m$  is linearly dependent on  $N_n$ . Dashed line shows the region where the fixed point is unstable and the solid line shows the region where it is stable. Black dots mark the parameter values used in (B) and (C). The crossover from unstable to stable occurs where  $\epsilon$  becomes comparable to the steady state value of  $I$ , i.e., where the degradation of  $I$  stops being saturated. **B.** Trajectory of the system in the  $I$ - $N_n$  phase plane, for  $\epsilon = 1 \times 10^{-4}$ , which converges to a stable limit cycle. **C.** Trajectory of the system, for  $\epsilon = 2 \times 10^{-4}$ , which converges to a stable fixed point.

The steady state value of  $N_n$  is now a solution to

$$(C - CN_n - N_n)^2 = \frac{BC\epsilon^2}{A} \frac{N_n^2}{\delta + N_n}.$$

The steady value of  $I$  can be calculated from the value of  $N_n$  using:

$$I = \frac{N_n\epsilon}{C - CN_n - N_n}.$$

In general, there are again two real solutions, one with  $C - CN_n - N_n > 0$  and the other with  $C - CN_n - N_n < 0$ . The latter results in a negative value for  $I$  and therefore is not an acceptable solution. Thus we are left with only one fixed point.

Linearizing the equations around the fixed point gives almost the same Hessian. The only difference is in one matrix element:  $J_{2,1} = 1$  instead of  $2N_n$ . Fig. S3 shows the stability of the fixed point as a function of  $\epsilon$ .